International Journal of Physical Sciences

Volume 12 Number 5 16 March , 2017

ISSN 1992-1950

Academic Journals

ABOUT IJPS

The **International Journal of Physical Sciences (IJPS)** is published weekly (one volume per year) by Academic Journals.

International Journal of Physical Sciences (IJPS) is an open access journal that publishes high-quality solicited and unsolicited articles, in English, in all Physics and chemistry including artificial intelligence, neural processing, nuclear and particle physics, geophysics, physics in medicine and biology, plasma physics, semiconductor science and technology, wireless and optical communications, materials science, energy and fuels, environmental science and technology, combinatorial chemistry, natural products, molecular therapeutics, geochemistry, cement and concrete research, metallurgy, crystallography and computer-aided materials design. All articles published in IJPS are peer-reviewed.

Contact Us

Editorial Office: ijps@academicjournals.org

Help Desk: helpdesk@academicjournals.org

Website: http://www.academicjournals.org/journal/IJPS

Submit manuscript online http://ms.academicjournals.me/

Editorial Board

International Journal of Physical Sciences

Table of Contents: Volume 12 Number 5, 16 March, 2017

ARTICLES

academicJournals

Vol. 12(5), pp. 52-59, 16 March, 2017
DOI: 10.5897/IJPS2016.4592
Article Number: 060876B63495
ISSN 1992 - 1950

http://www.academicjournals.org/IJPS

International Journal of Physical Sciences

Full Length Research Paper

Pressure and temperature effects on corona onset voltage in electrostatic precipitators

Fadhil Khaddam Fuliful

Physics Department, College of Science, Karbala University, Karbala, Iraq.

Received 16 December, 2016; Accepted 8 March, 2017

Corona onset voltage is one of the most important factors that determine the charging toxic particle in an industrial application. Electrostatic precipitators (ESP) remove the suspended particle with a gas inlet. This paper developed Peek's formula to estimate the maximum electric field near the discharge wire in corona discharge models, the values of maximum electric field and corona onset voltage near the discharge wires have been calculated for different values of pressure and temperature for confined gas in a region between the electrodes in ESP. The model uses finite difference method (FDM) to solve governing equations (Poisson's and current continuity equations) simultaneously. Computer simulation method uses FORTRAN program to estimate potential distribution and maximum electric field intensity. The calculated corona onset voltage values are compared with the calculated values of different models.

Key words: Corona onset voltage, corona discharge, electric field distribution, electrostatic precipitators.

INTRODUCTION

As far as the design of high voltage apparatus is concerned, the knowledge of the corona onset voltage, which is a fundamental aspect always challenges design engineers. Lately, this information has gained more importance in compact transmission line designs where the average E-field magnitude is naturally higher as compared to conventional structures (Olsen et al.,1997).

The globalization of the environmental pollution problems caused by the increase of industrial production will lead to the cleaning of the waste gases. The basic idea of electrostatic precipitators is charging the toxic particles such as CO_2, Nox by interring it. Electrostatic field drives the charged particles to collection on plates connected to earth. The dry plate-type (ESP) is used widely in industrial applications to control dust pollution (Nicolae et al., 2008). It is a new method used to calculate onset voltages in case of negative and positive corona, this method is based on considering electric field and pressure in adjacent surface of conductors. This algorithm is simulated for different pressure and radius of conductors. The configuration of conductors considered is stranded as overhead high transmission lines (Zangeneh and Gholami, 2005). The impact of various variables on corona power losses and corona onset

E-mail: Fadhil.Khaddam@yahoo.com.

voltages was determined, and DC and AC tests were performed at Fuat Kulunk high voltage laboratory of Istanbul Technical University (Eroncel et al., 2010). Investigation of corona onset was done, and different factors such as the electric field (E-field) distribution around the electrodes and their surface conditions were taken into account (Souza and Lopes, 2008). The corona inception voltage (CIV) of positive discharges in a typical wire-cylinder electrode arrangement in air was studied under high voltage DC application, finite element analysis (FEA) implemented. Numerical analysis was carried out on the electric field intensity along the wire-cylinder gap axis, in order to determine the inception voltage of each air gap and define its dependence on geometrical characteristics of the electrodes (Konstantios et al., 2013). A study on how onset voltage is influenced by the number of discharge wires, the wires radius and the spacing between wires and the collecting plates, the initiation of the corona discharge and electric field calculated using the charge simulation method was done (Ziedan et al., 2010). Theoretical investigation of onset voltage was described for negative corona on stranded conductors, the method of calculation is based on criterion developed for formation of repetitive negative corona (Trichel pulses), an accurate calculation of the electric field satisfied in the vicinity of stranded conductors, and the investigated gap is a three-dimensional field problem, to solve this problem, a new modification of the charge simulation technique is presented (EL-Bahy et al., 2007).

A pressure sensing unit is based on a unique corona discharge setup using symmetrical electrode arrangement with simultaneous positive and negative corona generation. The device generates stable corona discharge and enables reliable air pressure measurement in the range of 80 to 105 kPa, tested with five prototypes. Three governing parameters, namely electrode geometry, electrode distance and discharge current, were studied in relation to absolute pressure (Van Thanh et al., 2016a).

A miniaturized device generate ion wind flow with very low net charge. Both positive and negative ions are simultaneously generated from two sharp electrodes placed in parallel, connected to a single battery-operated power source. The two-electrode arrangement is symmetrical, where the electrode creating charged ions of one polarity also serves as the reference electrode to establish the electric field required for ion creation by the opposite electrode, and vice versa (Van Thanh et al., 2016b).

This paper aimed to evaluate the corona onset voltage in ESP depending on developing Peek's formula. A mathematical model employed Finite Difference technique to solve Poisson's and current continuity equations simultaneously also the developed formula for calculating the maximum electric field near the discharge wire. The equations programmed in FORTRAN. Corona onset voltage evaluated for different values of pressure and temperature at dust condition, also the influenced of discharge wires, the wires radius and the spacing between wires and collecting plates on the onset voltage calculated. The computed onset voltage values agreed reasonably with those measured experimentally

CORONA ONSET MODELS

Monitoring the temperature of the gas stream provides useful information on the performance in the ESP and gives useful ideas for diagnosing (maintenance and process operating conditions). The effect of temperature is most important as it relates to the resistivity of the particulate and is an indicator or excessive in leakage into the gas stream. Temperature can also have effects on gas properties such as the relative levels of current, the density and viscosity of the gas stream, as consequence of the particle migration parameters of charge particle also affected. There are several parameters that affect corona onset voltage in addition to the surface E-field, such as the ambient conditions, temperature, air pressure and relative atmospheric conditions. Prediction models of corona onset voltage were few (Olsen et al., 1997; Zangeneh and Gholami, 2005; Eroncel et al., 2010; Konstantios et al., 2013; Ziedan et al., 2010; EL-Bahy et al., 2007; Van Thanh et al., 2016c). Figure 1 shows the regions of corona discharge, the electric field intensity is high in glow region and decreases slowly towards the drift region and equal to zero in passive electrode.

In this paper, an iterative procedure was used to calculate maximum electric field intensity near the corona discharge wire. The model based on FDM was used in solving Poisson's and current continuity equations simultaneously after computing the initial electric field intensity due to the developed Peek's formula. FORTRAN programs are used for investigating electric field distributions along the gap distance (distance between discharge wire and ground plates for ESP), and corona onset voltage near the discharge wire. The boundary conditions needed for the solution of problem domain are value of applied voltage on the discharge wire (equal to the applied DC voltage), the zero potential on the collecting plate, the corona onset gradient on the discharge wire, E_c as given by Peek's formula and the estimations of potential distribution at all grid points for the problem domain evaluated due to Cooperman's equation.

If the wires are rough, marred, or specked with dust, as it commonly the case in practice, it is necessary to introduce the roughness factor (f) less than 1 and the values ranged from 0.5 to 0.7(James et al., 1995).

PEEK'S FORMULA

The empirical expression developed by Peek in 1929, for the critical

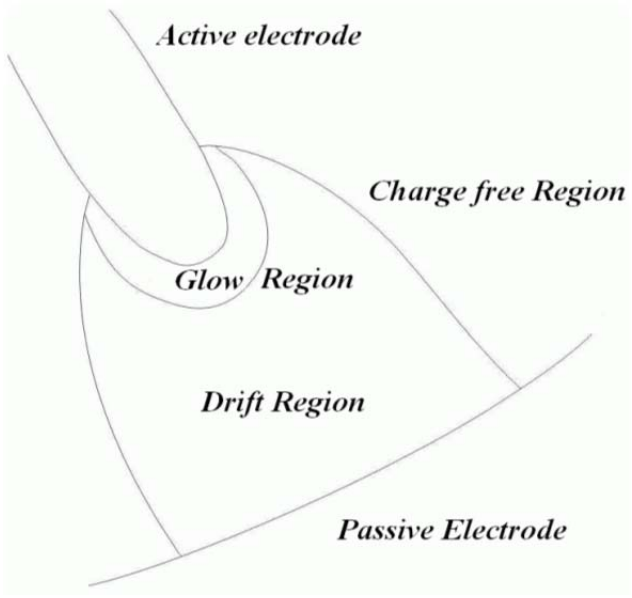

Figure 1. Schematic representation of the regions in corona discharge (Goldman et al., 1982).

E-field is the most widespread and widely used for various arrangements, although originally developed for concentric cylinder arrangements (Kuffel et al., 2000). Equation 1 shows Peek's formula to estimate corona onset as perceived by visual observations.

$$E_c = 31.\delta\,.f(1+0.308.(\delta.r)^{-0.5}) \quad (1)$$

Where E_c = critical E-field, δ = relative air density, *r* = conductor radius and *f* = roughness factor. (f = 1 for polished wires and δ=1 at NTP).

The corona onset voltage V_c may be obtained from the Equation below (James et al., 1995):

$$V_c = rE_c\, ln\frac{S_x}{r} \quad (2)$$

Where S_x is the distance between discharge wire and collecting plate.

Zaengl and Nyffenegger equation

Zaengl and Nyffenegger developed an analytical expression, rewriting Peek's formula in the form presented in Equation 3 (Kuffel et al., 2000):

$$(E_c/\delta)^2 - 2\left(\frac{E_c}{\delta}\right)E_\circ.\ln\left(\frac{E_c}{\delta.E_\circ}\right) - (E_\circ)^2 = \frac{42}{\delta r} \quad (3)$$

This expression was developed due to deviations obtained with Peek's formula for δ*r* > 1.

Field efficiency factor

Later on, the influence of the gap geometry was expressed in terms of the 'field efficiency factor" (FEF), also called "utilization factor" (Kalenderli et al., 2001) or its reciprocal, the "non-uniformity factor" (Qiu, 1986). The field efficiency factor (η) is the ratio between the uniform E-field for the gap length (E_{mean}) and the maximum E-field (E_{max}) at rod tip as shown in Equation 4.

$$\eta = E_{mean} \;/\; E_{max} \quad (4)$$

For simple structures, the maximum field is taken as the electrode surface, for complex electrode arrangement E_{max} may appear at any point on an electrode. The FEF measures the "degree of non-uniformity" of the arrangement: the closer it is to 1, the more uniform the field is in the arrangement.

$$\eta = (0.45.\frac{d}{r}.\ln(6.\frac{d}{r})/ln(\frac{d}{r}))^{-1} \quad (5)$$

Using curve-fitting techniques, an expression was suggested for η as a function of the ratio between the gap length (*d*) and electrode radius (*r*) (Qiu, 1986), this expression is presented in Equation 5. According to this factor η and the maximum E-field, the corona onset voltage (V_c) can be calculated due to Equation 6.

$$V_c = d.E_{max}.\eta \quad (6)$$

Where *d* is the gap length and E_{max} the maximum E-field value.

A new prediction model

Peek's formula does not considered the high Pressure and Temperature conditions because roughness factor value is one for polished wires. Therefor a new method based on considering high pressure and temperature near the surface of discharge wires in ESP investigated. This model simulated for different pressure and temperature values which are affected on density of the gas in the

Table 1. Simulated corona onset voltage using Peek's formula for different discharge wire and gap distance.

Wire radius (cm)	Gap Length (cm)	corona onset voltages (kV)
0.0129	3	4.188
	5	4.564
	7	4.811
0. 0392	3	7.071
	5	7.859
	7	8.379
0. 1879	3	14.988
	5	17.530
	7	19.204
0.1	3	11.113
	5	12.672
	7	13.697

Table 2. Simulated maximum E-field (kV/cm) near the discharge wire for different mathematical models.

Wire radius (cm)	Gap length (cm)	Maximum E-field (kV/cm)				
		Peek	Zaengl	Y.Qiu	FEM	FDM
0.0129	3	100.1	101.9	231.8	116.11	28.5
	5			272.2	98.0	20.7
	7			358.5	96.2	16.4
0. 0392	3	78.7	73.2	129.8	58.5	32.7
	5			141.5	54.2	24.5
	7			154.5	50.8	19.3
0. 1879	3	52.9	50.1	59.2	43.9	45.6
	5			62.9	39.9	27.7
	7			64.5	35.2	20.8

ESP, the objective of this work to develop the Peek's formula.

$$E_c = 31.\frac{T_0}{T}.\frac{P}{P_0}.f(1 + 0.308.(\frac{T_0}{T}.\frac{P}{P_0}.r)^{0.5}) \quad (7)$$

Where T_0 is the absolute temperature of room air or about 293°K, P_0 is the normal atmosphere pressure or 760 mmHg and T and P are actual temperature and pressure of gas for which δ is to be calculated.

RESULTS AND DISCUSSION

There are several important cases for which corona can occur, corona onset voltage is considered as a starting point for corona and it is difficult to measure these values experimentally, then theoretical study is necessary. A different empirical formula for calculating the voltage gradient are used and determination of corona onset voltage is useful, it is necessary to evaluate its values at ESP under dust loading.

Table 1 show values of corona onset voltage calculated according to Peek's formula at different values of gap distance, it's evident that corona onset voltage affected by discharge wire radius and gap distance, the computation happen under dust free conditions.

Table 2 shows the simulated maximum E-field (kV/cm) near the discharge wire for different mathematical models, the comparison shows that the simulated results gives agreement with other models in case of high values for wire radius (r=0. 0392 cm), the reduction of maximum

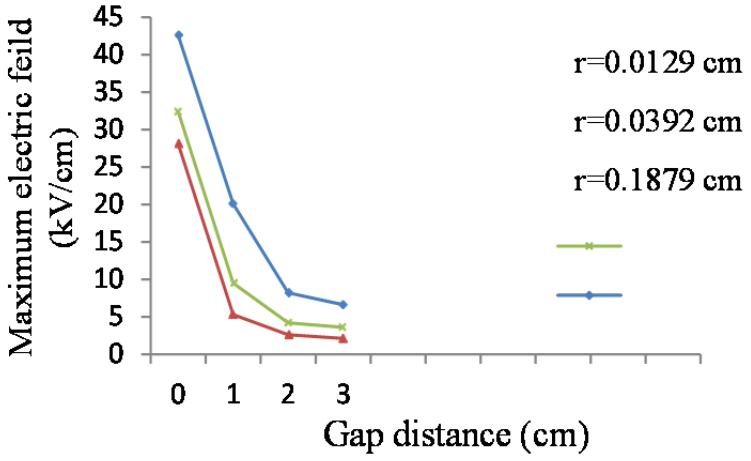

Figure 2. Maximum electric field distribution along the distance between discharges wire and ground plate (3 cm) for different wire radius.

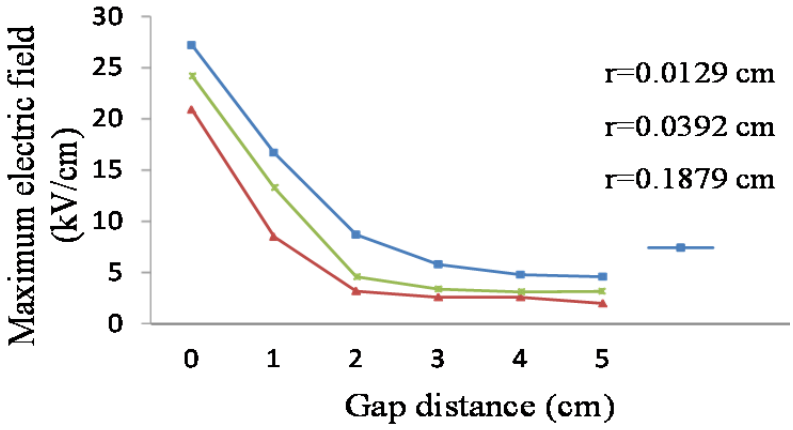

Figure 3. Maximum electric field distribution along the distance between discharges wire and ground plate (5 cm) for different wire radius.

electric values which are calculated in a new model related to the employed conditions (high pressure and temperature), while the other models used atmospheric conditions.

Figure 2 shows maximum electric field distribution along the gap distance equal to 3 cm (distance between discharge wire and ground collecting plate), the electric field have highest value near the discharge wire and decreases slowly towards the ground plate, this result investigate the basis of the ionization in corona discharge, the same manner of electric field distribution have been seen in Figures 3 to 4 at the gap distance (5 and 7 cm, respectively). The predicted results show that the effects of gap distance on corona onset voltage is weakly as shown in the Figures 2 to 4, but the effect of wire radius is strongly shown.

Tables 3, 4 and 5 show the effects of high pressure temperature on maximum electric field and corona onset voltage near the corona discharge wire in ESP, it is evident that the increased high pressure-temperature leads to decreases in corona onset voltage and maximum electric field. There are no effects of distance gap on maximum electric field but slightly effect on corona onset voltage but the radius wire still affects them.

Conclusion

In practice, measuring the corona onset voltage is difficult; therefore, mathematical models are important to evaluate its values. There are different models used for computing corona onset voltage of a gas in atmosphere conditions but dust conditions are poor in the study, the model which has been built in this work is useful for

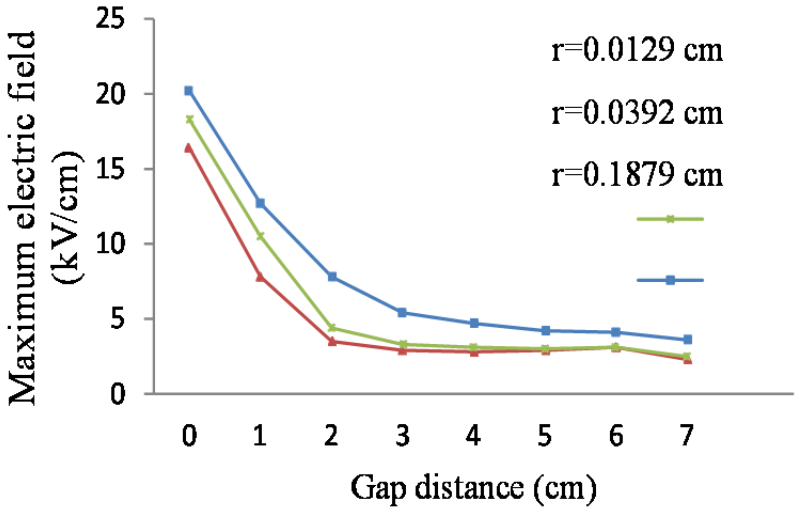

Figure 4. Maximum electric field distribution along the distance between discharges wire and ground plate (7 cm) for different wire radius.

Table 3. Simulated maximum E-field (kV/cm) and onset corona voltage (kV) for different values of high pressure-high temperature at wire radius r=0.0129 cm.

Wire radius (cm)	Gap distance (cm)	Pressure (kPa)	FDM		
			Temperature (K)	Maximum electric (kV/cm)	Onset voltage (kV)
0.0129	3	500	950	180	6.63
			1050	157	5.78
			1150	139	5.10
			1250	124	4.55
			1350	111	4.09
			1400	106	3.90
	5		950	180	7.23
			1050	157	6.30
			1150	139	5.56
			1250	124	4.96
			1350	111	4.46
			1400	106	4.25
	7		950	180	7.62
			1050	157	6.64
			1150	139	5.86
			1250	124	5.23
			1350	111	4.71
			1400	106	4.48

determining corona onset voltage for industrial ESP. Corona onset voltage is low in high pressure-temperature.

CONFLICT OF INTERESTS

The author has not declared any conflict of interests.

Table 4. Simulated maximum E-field (kV/cm) and onset corona voltage (kV) for different values of High Pressure-High temperature at wire radius r=0.0392 cm.

Wire radius (cm)	Gap distance (cm)	Pressure (kPa)	Temperature (K)	FDM	
				Maximum Electric (kV/cm)	Onset voltage (kV)
0.0392	3	500	950	122	10.90
			1050	107	9.62
			1150	95.17	8.54
			1250	85.34	7.65
			1350	77.19	6.92
			1400	73.63	6.60
	5		950	122	12.20
			1050	107	10.69
			1150	95.17	9.49
			1250	85.34	8.51
			1350	77.19	7.70
			1400	73.63	7.34
	7		950	122	13.01
			1050	107	11.40
			1150	95.17	10.12
			1250	85.34	9.07
			1350	77.19	8.21
			1400	73.63	7.83

Table 5. Simulated maximum E-field (kV/cm) and onset corona voltage (kV) for different values of high pressure-high temperature at wire radius r=0.1879 cm.

Wire radius (cm)	Gap distance (cm)	Pressure (kPa)	Temperature (K)		
				Maximum Electric (kV/cm)	Onset voltage (kV)
0.1879	3	500	950	79.65	Onset voltage kV
			1050	70.48	22.54
			1150	63.09	19.94
			1250	57.03	17.85
			1350	51.97	16.14
			1400	49.75	14.70
	5		950	79.65	14.07
			1050	70.48	26.34
			1150	63.09	23.32
			1250	57.03	20.88
			1350	51.97	18.87
			1400	49.75	17.20
	7		950	70.65	16.46
			1050	70.48	28.88
			1150	63.09	25.55
			1250	57.03	22.87
			1350	51.97	20.68
			1400	49.75	18.84

REFERENCES

EL-Bahy MM, Abouelsaad M, Abdel-Gawad N, Badawi M (2007). Onset voltage of negative corona on stranded conductors. J. Phys. D: Appl. Phys. 40:1-8.

Eroncel C, Ilhan S, Ozdemir A, Kaypmaz A (2010). Corona Onset Voltage and Corona Power Losses in an Indoor Corona Cage, Proceedings of the 14th International Middle East Power Systems Conference (MEPCON'10), Cairo University, Egypt, December 19-21, 2010, Paper ID 286.

Goldman M, Sigmond RS, Nicole R (1982). Corona and Insulation. IEEE Trans. Electr. Insul. EI-17(2).

James HT, Phil AL, Toshiaki Y, David WC (1995). Electrostatic Precipitators, Research Triangle Institute 1995.

Kalenderli Ö, Önal E, Altay Ö (2001). Computing the Corona Onset and the Utilization Factor of Rod-Plane Electrode by Using Charge Simulation Method. Electrical Insulation Conference and Electrical Coil &Winding Conference, October 2001. Manufacturing.

Konstantios NK, Antonios XM, Emmanouil DF (**2013**).Finite element analysis method for detection of the corona discharge inception voltage in a wire-cylinder arrangement. Recent Advances in Finite Differences and Applied & Computational Mathematics, Mathematics and Computers in Science and Engineering Series, 12:188-193.

Kuffel E, Zaengl WS, Kuffel J (2000). High Voltage Engineering Fundamentals. Second Edition, 2000.

Nicolae PG, Vaida V, Iagar A, Dinis CM (2008). Improvement of Technological and Electric Performances for Plate Type Electrostatic Precipitators with Three Sections. Wseas Trans. Power Syst. 3(8).

Olsen RG, Phillips DB, Pedrow PD (1997). Extrapolation of a corona Streamer1 Onset criterion to general convex conductor surface" 10th International on High Voltage Engineering, August 1997.

Qiu Y (1986). Simple Expression of Field Non uniformity Factor for Hemispheric ally Capped Rod-Plane Gaps. IEEE Trans. Electr. Insul. EI-21(4).

Souza AL, Lopes IJS (2008). Corona Onset Models: A Computational and Experimental Evaluation. In Electrical Insulation and Dielectric Phenomena, 2008. CEIDP 2008. Annual Report Conference on (pp. 698-701).

Van Thanh D, Bui TX, Tran TT, Phan CD, Terebessy HT (2016c). Corona Based Air-Flow Using Parallel Discharge Electrodes. Exp. Therm. Fluid Sci. 79:52-56.

Van Thanh D, Thien XD, Tibor T, Tung TB (2016b). Bipolar corona discharge based air flow generation with low net charge. Sens. Actuators A. 244:146–155.

Van Thanh D, Tung TB, Thien XD, Tibor T (2016a). Pressure sensor based on bipolar discharge corona configuration. Sens. Actuators A 237:81-90.

Zangeneh A, Gholami A (2005). A New Method for Calculation of Corona Inception Voltage in Stranded Conductors of Overhead Transmission Lines, 20th International Power System Conference, 2005.

Ziedan H, Sayed A, Mizuno A, Ahmed A (2010). Onset Voltage of Corona Discharge in Wire-Duct Electrostatic Precipitators. Int. J. Plasma Environ. Sci. Technol. 4(1).

academicJournals

Vol. 12(5), pp. 60-73, 16 March, 2017
DOI: 10.5897/IJPS2016.4595
Article Number: 687949963497
ISSN 1992 - 1950

http://www.academicjournals.org/IJPS

International Journal of Physical Sciences

Full Length Research Paper

Hydrogeochemical investigation and characterization of shallow groundwater within Ankpa Town, North Central Nigeria

Akpah F. A.[1], Onwuka S. O.[2] and Oha I. A.[2]*

[1]Department of Earth Sciences, Kogi State University, Anyigba, Nigeria.
[2]Department of Geology, University of Nigeria, Nsukka, Nigeria.

Received 23 December, 2016; Accepted 8 March, 2017

Physico-chemical analysis of groundwater samples from Ankpa, north central Nigeria was carried out to investigate the quality of the water for drinking and irrigation purposes. The results revealed water of average low pH, indicating slightly acidic conditions of the water. The water is soft, and it is characterized as Na^++K - HCO_3 type. It is good for drinking and other domestic uses. Four indices were evaluated from the groundwater chemistry in order to establish the suitability of the water for irrigation purposes. They are the sodium adsorption ratio (SAR), the percentage sodium (%Na), the magnesium hardness (MH) and the permeability index (PI). The SAR values range from 0.86 to 11.19, with an average of 5.68. The interpretation indicates that the groundwater is good to excellent for irrigation. It further shows that over 90% of the samples can be classified as S1 waters, with no alkali hazard anticipated for the crops grown with the water. The range of the %Na in the groundwater in this study is between 16.28 and 73.97, with an average value of 51.27. This shows that the water ranges from excellent to doubtful for irrigation. The magnesium hardness (MH) in the groundwater ranges from 2.05 to 41.04%, with an average of 20.35%. This indicates that the entire water is safe for use for irrigation purposes. The chloride and sulphate concentrations in the groundwater indicate that the water is excellent for irrigation. However, the permeability index shows completely opposite conditions in the area, with all samples with values above 75.

Key words: Irrigation, physico-chemical analysis, water types, hydrochemical facies, Anambra Basin.

INTRODUCTION

The chemical composition of groundwater and the water types found in an environment are determined greatly by the composition of the water of precipitation, local geology, types of mineral found in the environment through which the recharge and groundwater flows. Other determinants include anthropogenic activities such as mining and waste disposal, as well as climate and topography. The quality of water in turn determines its usability for domestic, industrial and agricultural purposes. The inability of the state-owned Water Board to

*Corresponding author. E-mail: ifeanyi.oha@unn.edu.ng.

supply clean, treated water has led the residents of Ankpa to resort to other water sources, such as hand dug-wells and untreated surface water sources, especially the Mabolo River (the local name for the Anambra River).

The population of Ankpa town, the political and administrative headquarters of Ankpa Local Government Area has greatly grown since the creation of Kogi State in 1991. Rise in population has often had its inherent adverse consequences on the environment, of which among the chief is the generation of large volumes of domestic waste which are difficult to manage. This is the case in Ankpa. Domestic wastes are disposed either in open dumps or in the Mabolo River due to absence of sanitary waste disposal systems within the town. These conditions place a great concern on the quality of the water used for domestic purposes in Ankpa. The poor sanitary conditions in the town have continued to expose both groundwater and surface water to possible contamination, consequent from the direct washing of waste materials by seasonal rain water into the River Mabolo to the leaching of dissolved matter leaching into the groundwater system. The Mabolo (Imabolo) river serves as an important source of water supply in Ankpa, because of lack of reticulated public water supply. Obeta et al. (2015a, b) have reported the poor quality of the Mabolo (Imabolo) river for consumption and other domestic purposes. The river might be making a very important contribution to the recharge of the shallow sandy aquifer, thereby contributing further to the degradation of the groundwater. Leachate from open dumps has been found to contribute significantly to the quality of water in some Nigerian cities with shallow groundwater systems (Onwuka et al., 2004, 2013a; Ehirim et al., 2009; Omonona et al., 2014). Obeta and Ocheja (2013) had reported unwholesome quality of groundwater in Ankpa, which is attributable to conditions related to poor hygienic conditions in the area.

Evaluation of groundwater for irrigation purposes has been carried out by many researchers, and several standards for the suitability of irrigation water have been set by many bodies. Examples include the works by Doneen (1964), Stuytzand (1989), Hagras (2013), Bhuiyan et al. (2015), and Mirza et al. (2014).

Location and geomorphology of the study area

Ankpa township is located within latitude 7° 23' N to 7° 25' N and longitude 7° 37' E to 7° 39' E in the central part of Ankpa local government area of Kogi State, north central Nigeria (Figure 1). The town lies on a gently undulating plateau bisected by the River Anambra valley. The river drains most of the area flowing from north to south of Ankpa and abuts the eastern side of the town. This may have been responsible for developments in the area, tending towards the western part of the river valley as residential and infrastructural developments as well as commercial activities are more concentrated in the western flank of the river.

Climatic conditions in the area

The climate of Ankpa is that of tropical hinterland of Nigeria (Iwena, 2012). The area experiences two main seasons, namely, wet and dry season. The wet season commences in May and lasts till October/November. Ankpa receives annual rainfall of up to 1000 mm. Dry dust-laden Harmattan wind blows from the north-east into the area during the dry season starting from November to April. Temperatures in the area range from 17 to 34°C. Average monthly relative humidity recorded in the area for the same year ranged between 65 and 94%. Ankpa belongs to the Guinea Savannah vegetation of Nigeria (Iwena, 2012). Cash crops such as palm trees and cashew (*Anacardium occidentale*) are commonly grown in areas directly overlain by the Ajali Sandstone, because of the pedological peculiarities of the areas (Nwajide, 2013); and particularly, Ankpa area is one of the largest producers of cashew in Nigeria.

Geology of the area

Ankpa lies within the northern flank of the Anambra sedimentary basin of Nigeria. The Anambra Basin is a funneled shaped basin (Figure 2) whose formation commenced with the Mid-Santonian deformation in the Benue Trough, displacing the major depositional axis westward, thereby leading to the formation of the basin (Obaje, 2009). The post deformational sedimentation in the Lower Benue Trough therefore constitutes the Anambra basin. Sedimentation in the basin commenced with the Campanian-Maastrichtian shales of the Enugu and Nkporo Formations, overlain by the coal measures of the Mamu Formation followed by the Cretaceous sandstones of the Ajali and Owelli Formations, which in turn are overlain by the Imo and Nsukka shale Formation deposited in the Paleocene. The uppermost layer consists of the Eocene Nanka Sandstone.

The Ajali Formation, which is also known as the Ajali Sandstone, is the most important aquiferous sandstone formation in the Anambra Basin, with thickness exceeding 300 m to about 450 m (Offodile, 2002). Ankpa area is located on the Ajali Formation. The Formation outcrops around Idah-Ankpa and Nsukka Plateaux, marking the Idah-Enugu Escarpment and covering most of Idah, Ankpa and Nsukka. According to Nwajide (2013), the characteristic scenery of most areas is underlain by the Ajali Sandstone is that of a gently undulating topography or flat plains, punctuated by inselbergs, which are lone mounds of erosional resistors. The vast terrain called the Ankpa plateau, which emerges southwards with the plains west of Enugu, exemplifies its characteristics. The

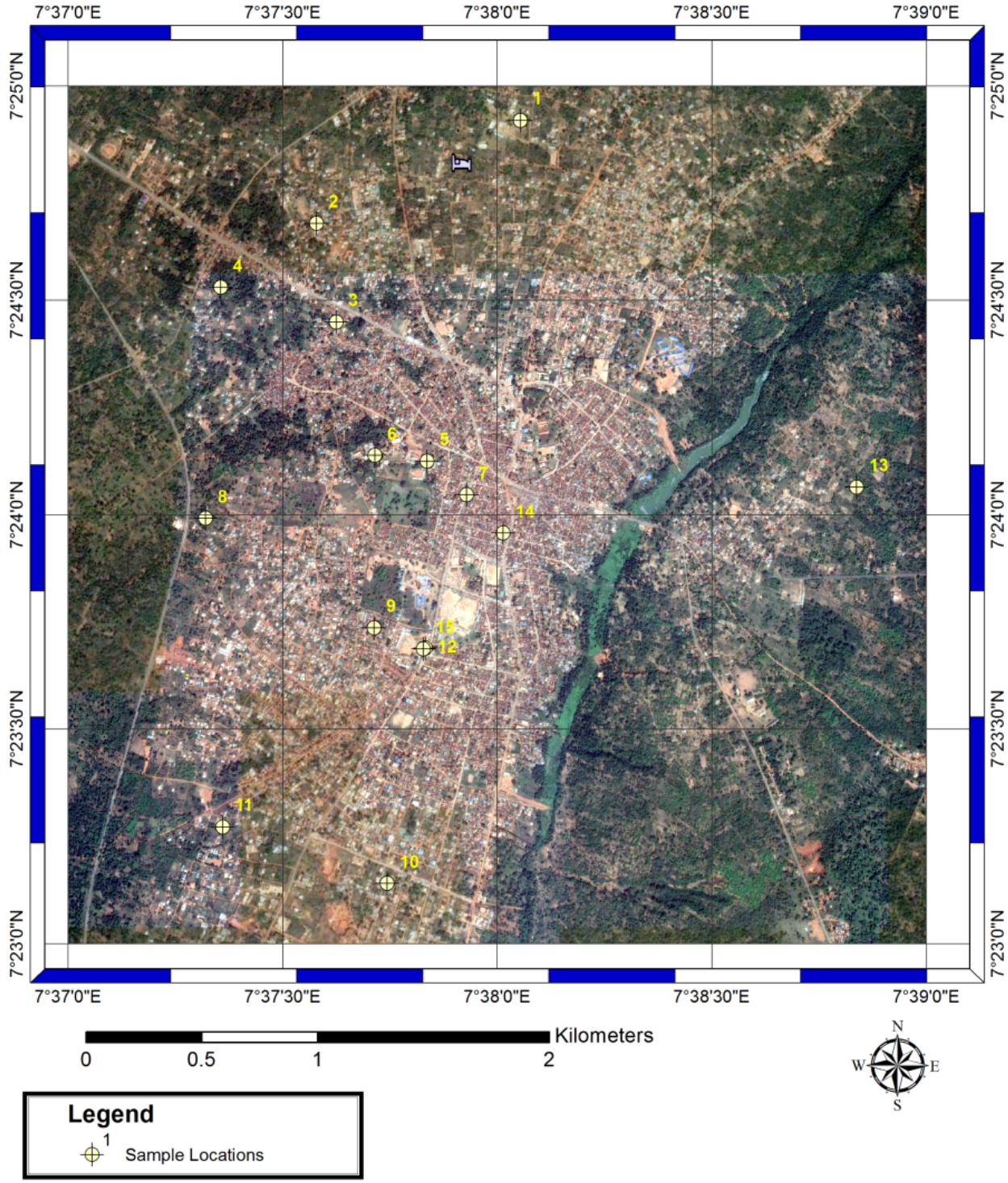

Figure 1. Google earth image of Ankpa township showing sample locations.

formation consists of coarse grained sandstones with thin lenticular shales beds of grit and pebbly gravel. The aquiferous sands are friable, poorly sorted and typically whitish at depth. The Ajali sandstone tends to be ferruginized as a result of weathering (Kogbe, 1989) and laterite is virtually the topsoil in all areas underlain directly by the formation. Lateritic thicknesses up to 40 m have been reported in areas south of Ankpa (Ezeigbo and Ozoko, 1989).

The drainage density on terrains underlain by the Ajali

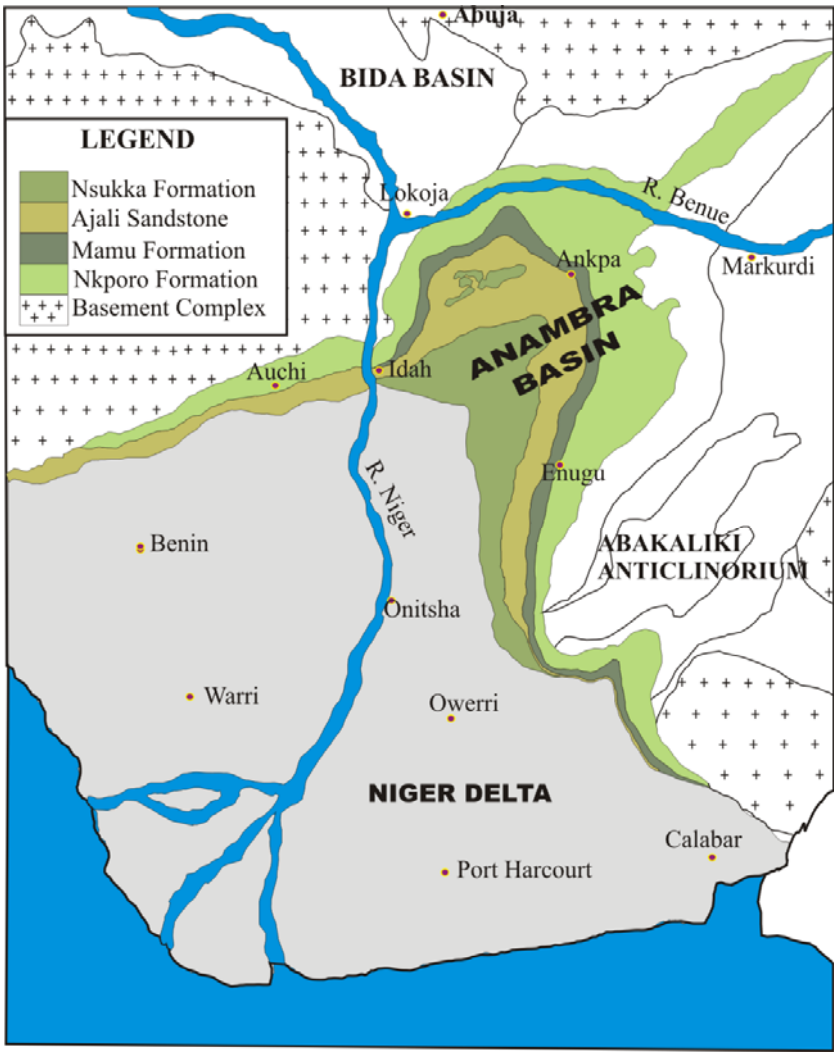

Figure 2. Geological sketch map of the Anambra basin modified from Obaje (2009).

Sandstone is generally low. This may be due to the ease of infiltration that greatly reduces overlain flow. Another perspective is that the water table is generally low, again due to ease and great depth of infiltration, such that springs are rare and rivers are therefore rarely generated (Nwajide, 2013).

The existence of several shallow perennial hand-dug wells in Ankpa is an evidence of the existence of shallow groundwater in the area. Some wells are as shallow as 10 m. This is not a reflection of the regional aquifer in the Ajali Sandstone, which has been reported to be up to 100 m in places (Ezeigbo and Ozoko, 1989). It is not the interest of this work to investigate the aquifer types in Ankpa. But the existence of shallow hand-dug wells that serve the water needs of the people portends health threat to the people because shallow aquifers are vulnerable to pollution (Onwuka et al., 2004, 2013a; Ofoma et al., 2008).

METHODOLOGY

The investigation commenced with the utilization of global positioning systems (GPS) to mark out the locations of the fifteen (15) water wells within the study area (Table 1). This was followed by collection of the groundwater samples from the wells in pairs of plastic and glass bottles. One set of samples was used for the cation determination and the other set for anion determination. At the point of sampling, physical parameters such as acidity (pH), temperature and electrical conductivity that change rapidly with time were measured shortly after water withdrawal. Two (2) drops of concentrated Trioxonitrate (v) acid were added to each of the samples in the plastic bottles for homogenization and prevention of absorption/adsorption of trace metals to the walls of the container (Schroll, 1975). The treated samples were subsequently used to determine the concentration of the following cations and heavy metals: Na^{+}, K^{+}, Ca^{2+}, Mg^{2+}, Fe^{2+}, Mn^{2+}, and Pb^{2+}. The samples in the glass bottles were used to determine the concentration of the following anions: SO_4^{2-}, Cl^{-}, NO_3^{-}, and HCO_3^{2+}.

Determination of concentration of Ca^{2+}, Fe^{2+}, and Pb^{2+} was done using A.A.S. –Buck Scientific Model 210 VGP. Flame analysis was

Table 1. Results of physical and chemical analysis on water from the study area.

Sample No.	1	2	3	4	5	6	7	8	9	10	11	12	13	14	15
Temperature (°C)	28	28	28	28	29	30	29	30	30	30	30	30	30	30	30
PH	5.8	5.8	5.8	5.1	5.0	6.6	6.2	6.4	5.2	5.1	5.2	6.2	6.4	5.2	6.0
TDS (ppm)	22	47	310	147	1950	1425	151.3	153	1047	91	108	61	821	65	575
Cations (ppm)															
Na^+	8.12	32.41	95.0	9.35	271.3	220.1	224.7	44.37	220.7	49.69	42.21	45.01	207.4	28.71	143.0
K^+	3.22	8.15	108.3	64.41	455.1	353.9	378	41.15	171.4	10.54	93.0	3.65	247.6	13.0	164.2
Mg^{2+}	0.21	0.72	3.15	2.20	3.87	3.77	3.82	2.07	3.71	2.02	0.93	1.03	3.64	0.19	3.582
Mn^{2+}	0.03	0.05	0.11	0.02	0.78	0.03	0.87	0.012	0.01	0.18	0.02	0.06	0.02	0.01	0.08
Fe^{2+}	0.02	0.04	0.10	0.03	0.19	0.02	0.10	0.02	0.03	0.04	0.11	0.04	0.06	0.15	0.04
Pb^{2+}	0.07	0.08	0.07	0.03	0.03	0.02	0.03	ND	ND	0.06	0.08	0.06	0.03	0.16	0.15
Ca^{2+}	4.52	8.11	7.63	5.21	65.30	42.00	56.41	8.21	31.22	6.51	4.22	29.73	20.01	15.32	10.54
Anions (ppm)															
SO_4^{2-}	6.60	4.41	4.70	4.65	4.55	4.32	4.35	4.20	4.40	5.10	4.50	4.30	4.20	4.40	4.35
Cl^-	0.07	0.07	0.11	0.43	0.28	0.28	0.065	0.07	0.19	0.07	0.07	0.05	0.25	0.06	0.19
NO_3^-	7.10	7.60	12.0	14.1	26.85	23.8	17.25	4.40	16.2	2.20	1.80	9.30	12.0	1.70	16.00
HCO_3^{2+}	19.8	98.45	220	143.2	176.7	180.3	123.9	96.8	142.4	84.32	122.5	181.1	74.51	212.4	179.6

used to determine the concentrations of Na^+ and K^+. Concentration of SO_4^{2-} was determined using the colometric method while concentrations of Cl^- and HCO_3^- were determined using titrimetric methods. Determination of NO_3^- was done using a UV spectrophotometer. Total dissolved solids (TDS) were determined by evaporation technique involving gravimetric analysis, and this method has a detection limit of approximately 10 mg/L.

The results of the physico-chemical analysis of the water samples were evaluated to determine the quality of the water for both domestic and agricultural uses. For example, the potability of the water was determined by evaluating the hardness of the samples, and also by comparing the concentration levels of the parameters with the World Health Organisation (WHO) standards for drinking water. The parameters were also evaluated to determine and classify the water type (facies), and also to evaluate the corrosion and encrustation potentials of the water, as well as its acceptability for irrigation purposes. Groundwater characterization into facies was done by the use of Stiff pattern diagrams and Piper trilinear diagrams. Stiff pattern diagrams facilitate rapid comparison of results using absolute concentrations in milliequivalent per litre. The patterns were plotted by converting the measured absolute concentrations of the cations and anions to milliequivalent per litre followed by plotting of concentrations of the cations to the left of a vertical zero axis and the anions to the right of the same axis (Todd and May, 2005). For the Piper trilinear diagram, concentrations of major cations expressed as percentages of total cations in milliequivalent per litre were plotted as single plots on a left triangle while that of anions was plotted on a right triangle. The two plots were projected into a central diamond shaped area parallel to the upper edges of the central area.

Total hardness of the water, H_T, was determined using the Todd and Mays (2005) relationship:

$$H_T = 2.5\,[Ca^{2+}] + 4.1[Mg^{2+}]\ \text{mg/L} \quad (1)$$

The irrigation characteristics evaluated are the concentration of sodium in the water, the magnesium hardness (MH), and the permeability index (PI) of the soil. The concentration of sodium in the water was used to determine the sodium adsorption ratio (SAR) and the percentage sodium (%Na) in the water. The SAR was calculated using the expression of Todd and Mays (2005), as given in Equation 2:

$$SAR = \frac{Na^+}{\sqrt{(Ca^{2+} + Mg^{2+})/2}} \quad (2)$$

The %Na was calculated as expressed by Sadashivaiah et al. (2008) and Hagras (2013), in Equation 3:

$$Na\% = \frac{Na^+}{Na^+ + Ca^{2+} + Mg^{2+} + K^+} \quad (3)$$

Table 2. Concentrations of major cations and anions in (mg/L).

Sample	1	2	3	4	5	6	7	8	9	10	11	12	13	14	15
Na^+	8.12	32.41	95.0	9.35	271.3	220.1	224.7	44.37	220.7	49.69	42.21	45.01	207.4	28.71	143.0
K^+	3.22	8.15	108.3	64.41	455.1	353.9	378	41.15	171.4	10.54	93.0	3.65	247.6	13.0	164.2
Ca^{2+}	4.52	8.11	7.63	5.21	65.30	42.0	56.41	8.21	31.22	6.51	4.22	29.73	20.01	15.32	10.54
Mg^{2+}	0.21	0.72	3.15	2.20	3.87	3.77	3.82	2.07	3.71	2.02	0.93	1.03	3.64	0.19	3.582
SO_4^{2-}	6.60	4.41	4.70	4.65	4.55	4.32	4.35	4.20	4.40	5.10	4.50	4.30	4.20	4.40	4.35
Cl^-	0.07	0.07	0.110	0.43	0.28	0.28	0.065	0.07	0.19	0.07	0.07	0.05	0.25	0.06	0.19
HCO_3	19.8	98.45	220	143.2	176.7	180.3	123.9	96.8	142.4	84.32	122.5	181.1	74.51	212.4	179.6

The magnesium hardness (MH) is calculated with Equation 4, according to Szabolcs and Darab (1964), where the concentrations are meq/l. The permeability index (PI) is calculated according to Kacmaz and Nakoman (2010), as given in Equation 5.

$$MH = \frac{Mg^{2+}}{Ca^{2+} + Mg^{2+}} \times 100 \quad (4)$$

$$PI = \frac{Na^+ + \sqrt{HCO^-_3}}{Ca^{2+} + Mg^{2+} + Na^+} \quad (5)$$

The residual sodium bicarbonate (RSBC) is given as in Equation 6, after Gupta (1983):

$$RSBC = HCO_3^- - Ca^{2+} \quad (6)$$

RESULTS AND DISCUSSION

The location of wells where samples collected and results of the field and laboratory measurements on the water samples are shown in Table 1. Table 2 shows the values of the chemical parameters in both mg/l and meq/l, along with some average values. The measured temperature of water (between 28 and 30°C), indicates that the area is warm at the time of measurement since temperature is a representation of the degree of hotness/coldness of the area at the time of sampling.

The pH values for groundwater within the area range from 5.0 to 6.6. These values indicate that water from the area is slightly acidic. This value agrees with Freeze and Cherry (1979) assertions on hydrogeochemical sequences and facies, that rainwater in non-urban, non-industrial areas have pH values generally between 5 and 6.

Some of the samples had slight taste which could be as a result of dissolved substances. For shallow wells, particles carried by rainwater while infiltrating underlying formations may not be well filtered out before making contact with the aquifer.

TDS in the groundwater from the area ranged from 22 to 1950 mg/L. Based on Carroll (1962) groundwater classification, 80% of the water samples from the study area with TDS between 22 and 821 mg/L can be classified as fresh water while 20% of the samples with TDS between 1047 mg/L and 1950 are brackish. In the course of movement, there may be some localized contact/dissolution of sodium salt (as indicated by the water type) in the area responsible for the 20% brackish water.

Though a detailed study of corrosion was not carried out, the few corrosion parameters measured in the groundwater were used to assess the corrosion potentials of groundwater in the area. The implications of the acidity (pH 5-6) and warm temperature of groundwater (between 28 and 30°C) in combination with TDS >1000 mg/L in about 20% of samples from the area is that groundwater from the area is capable of corroding metals, especially in the presence of other parameters like dissolved oxygen (not determined). A combination of any two corrosion parameters such as pH <7, TDS >1 000 mg/L, warm temperature, HCO_3 > 50 mg/L and DO are required for corrosion to take place (Johnson, 1975).

Water type

Characterization of groundwater in Ankpa, using the Stiff pattern, Piper trilinear and Gibbs diagrams, are as shown in Figures 3, 4 and 5, respectively. These diagrams facilitate rapid comparison of results using the absolute concentration in Meq/l. The Stiff patterns can be a relatively distinctive method of showing water composition differences and similarities (Hem, 1985).

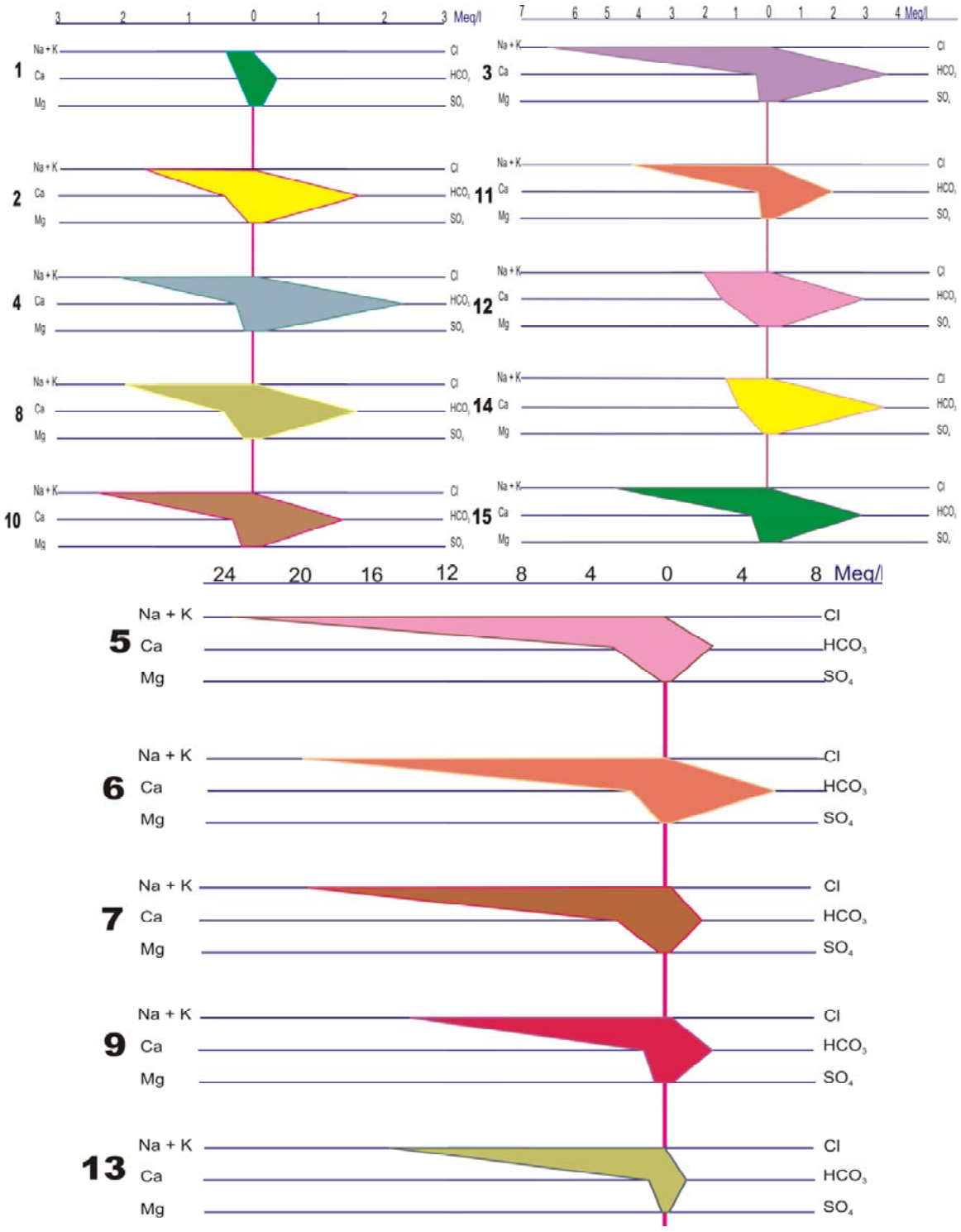

Figure 3. Stiff diagrams showing the dominant water types in Ankpa Township.

Those with similar qualities tend to plot together as a group.

The size of the pattern is approximately equal to the total ionic content (Hounslow, 1995). Apart from the pattern for sample 1, the Stiff patterns look similar and suggest no significant difference in the values of the TDS in the water samples, the shapes also suggest that the water samples are of the same source, with Na^{+} and HCO^{3}- as the dominant cation and anion, respectively (Onwuka et al., 2013b). The order of dominance for

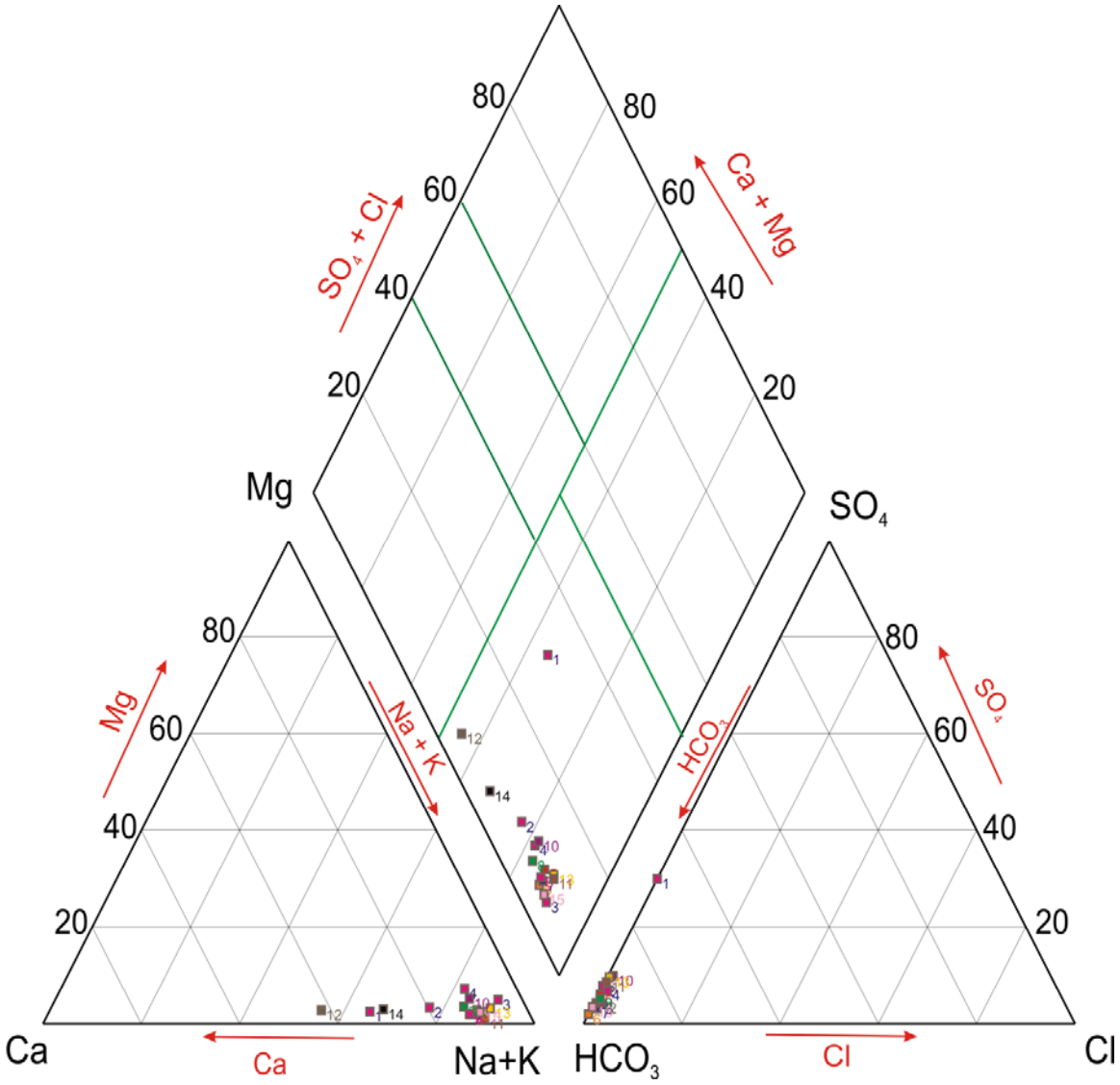

Figure 4. Piper trilinear diagram for classification of anion and cation groundwater facies in groundwater.

cations is $Na^{+}+K^{+} > Ca^{2+} > Mg^{2+}$, while that of anions is $HCO_3^{-} > SO_4^{2-} > Cl^{-}$.

Piper diagram can be used to determine water type, hydrochemical facies and ion exchange (Hounslow, 1995; Freeze and Cherry, 1979). The diamond part of Piper diagram may be used to characterize waters of different types (Hounslow, 1995). Water plotted at the lower corner of the diamond is primarily composed of alkali carbonates ($Na^{+}+k^{+}$ & $HCO_3^{-}+ CO_3^{2-}$) and can be classified as Sodium/Potassium Bicarbonate type. All the cations in the water samples plotted within the sodium and potassium section of the Piper trilinear plot, while the anions plotted within the bicarbonate section of the plot is as shown in Figure 4. This implies that the water is $Na^{+}+K$ - HCO_3 type and is in agreement with the results of the Stiff diagrams. This type of water can be described as juvenile water. It has low concentration of calcium and magnesium. The main source of such water is rainfall. The pH of the groundwater falls within the range of pH of water of precipitation.

Hydrochemical facies are dintinct zones that have cation and aniom concentrations described within defined concentration categories (Freeze and Chery, 1979); and designation of the facies is based on the manner suggested by Back (1961) and Back and Hanshaw (1965), in which facies are designated according to the domain in which they occur on the segments of a Piper diagram. On the basis of this subdivision, the groundwater in Ankpa belongs to the Sodium-Potassium facies and Bicarbonate facies. Clay minerals can have high cation-exchange capacities and may exert a considerable influence on the proportionate

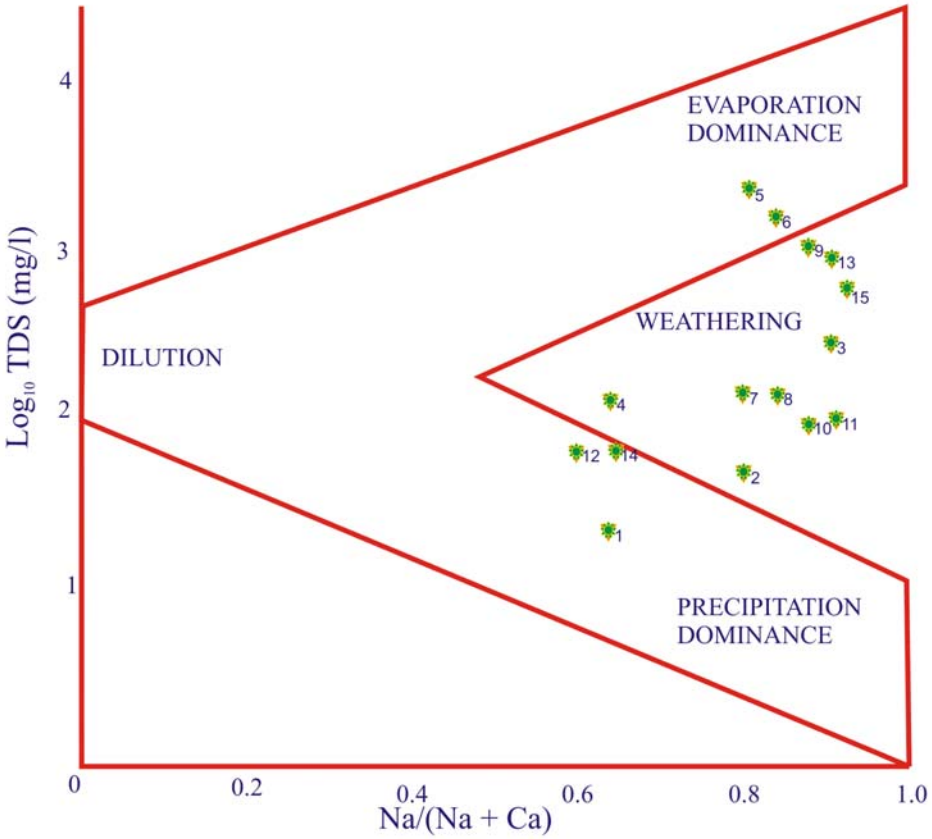

Figure 5. Gibb's diagram for water samples 1 to 15.

concentrations of the different cations in the water associated with them (Hem, 1985).

The Piper diagram clearly shows that cation exchange softening has increased the Na concentration at the expense of Ca and Mg concentrations. The Piper diagram also suggests that sulphate reduction may have taken place. Sulphate reduction is a kind of groundwater reaction that causes bicarbonate to increase, partly at the expense of sulphate. This reaction is caused by anaerobic bacteria (Hem, 1985).

The Gibbs (1970) diagram shows the mechanisms controlling groundwater chemistry, considering evaporation, dilution, weathering and precipitation. Most of the water samples from Ankpa plotted within the region of weathering, indicating more rock-dominated influence as opposed to evaporation, dilution and precipitation. This indicates that the water may have undergone possible extensive interaction with the geologic material underlying the area (Olayinka and Olayiwola, 2001; Tijani, 2003; Wang et al., 2004; Rao, 2006). Weathering is caused by the interaction of rocks with the atmosphere and hydrosphere, and can give rise to different products such as hydrolysates which are secondary products of the chemical breakdown of aluminosilicates, such as feldspars which are made up of clay minerals (Hounslow, 1995). Clay minerals are one of the major sources of cations like Na^+, K^+, Mg^+ and Ca^+ (Todd and Mays, 2005). These cations are common in the groundwater.

Hardness

The results of hardness of groundwater determined using divalent metallic cations responsible for hardness in groundwater in the study area, mainly calcium and magnesium is, shown in Table 3. Based on the Linsley et al. (1992) hardness classification of water (Table 4), only 3 samples, representing 20% of the water, are hard, with one (sample 5) tending to very hard water. The moderate hardness in Locations 9, 12 and 13 can be attributed to the closeness of the wells to a massive open refuse dump that has accumulated for over 20 years with leachate flowing into the sandy soil and possibly infiltrating into groundwater.

The water quality for irrigation

Quality of irrigation water is determined by its chemical composition and the conditions of use (Hussain et al., 2010).

Table 3. Hardness of groundwater from study area.

Sample	1	2	3	4	5	6	7	8	9	10	11	12	13	14	15
Ca^{2+}	4.52	8.11	7.63	5.21	65.30	42.00	56.41	8.21	31.22	6.51	4.22	29.73	20.01	15.32	10.54
Mg^{2+}	0.21	0.72	3.15	2.20	3.87	3.77	3.82	2.07	3.71	2.02	0.93	1.03	3.64	0.19	3.582
Hardness	12.16	23.227	31.99	22.045	179.117	120.457	156.687	29.012	93.276	29.4252	14.363	78.548	64.949	39.079	41.0362

Table 4. Hardness classification of water (Linsley et al., 1992).

Hardness (mg/L)	Water class	Percentage of sample
<15	Very soft	13.3
15 - 60	Moderately hard	46.7
61- 120	Hard	20.0
121 - 180	Very hard	20.0
>180	Very hard water	0.0

Two types of salt problems may exist in water: those associated with the total salinity and those associated with sodium (Fipps, 1969). Soils may be affected only by salinity or by a combination of salinity and sodium. Soil containing large proportions of sodium, with carbonate as the predominant anions is termed as alkali soil, whereas with chloride or sulphate as the predominant anions the soil is termed as saline soil. Both the spoil types will not support plant growth (Brindha et al., 2014). Saline soils are soils with high levels of total salinity. Saline conditions often result in “physiological” drought, where the soil is rendered impermeable, and though the field appears to have plenty of moisture, the plants wilt because the roots are unable to absorb water. Water with high salinity is toxic to plants and poses a salinity hazard (Fipps, 1969).

The other type of salt problem in water, known as sodium hazard, or alkalinity hazard, is the relative proportion of sodium to other principal cations. It is one of the most important characteristics in determining the quality of water for irrigation (Sadashivaiah et al., 2008). In this work, two aspects of sodium hazard of the water in Ankpa area are considered as the Na% and sodium adsorption ratio (SAR). The sodium adsorption ratio is used to predict the potential for sodium to accumulate in the soil, which would result from continued use of sodic water (Al-Tabbal and Al-Zboon, 2012). It is a measure of the tendency of sodium ion (Na^{+}) to displace calcium ion (Ca^{2+}) in the irrigation water due to its high position on the table of electrochemical series (Uzoije et al., 2015). This implies that more of sodium ions are readily available in the water as considerable amount of calcium is displaced. This condition produces adverse effects on the soil’s physical conditions and consequently on the crops, leading to a situation reported as sodicity or sodium hazards (Ayers and Westcot, 1985, 1994; Uzoije et al., 2015). High SAR in irrigation water makes the soil hard, compact and impervious (George, 1983), and results in water-logged soil conditions (Misstear et al., 2006), with its related plant diseases which include stunted growth and leaf burnt (Uzoije et al., 2015). In contact with soils, sodium reacts and reduces the permeability of the soils thereby supporting little or no plant growth. The results of SAR calculated for groundwater in the study area are shown in Table 5. The SAR values range from 0.86 to 11.19, with an average of 5.68. Table 6 shows that apart from sample 13 whose water is just good, fourteen (14) of the samples, constituting more than 90%, are excellent for irrigation, with respect to the sodium absorption ratio classification (Richard, 1954). Table 6 also shows the classification of the alkalinity hazard (Al-Tabbal and Al-Zboon, 2012), which indicates that all the samples, apart from Sample 13 fall in the low sodium class (S1). Sample 13 falls in the S2 class. The implication is that no alkali hazard is anticipated to crops grown

Table 5. Irrigation characteristics of groundwater in Ankpa.

Sample	1	2	3	4	5	6	7	8	9	10	11	12	13	14	15	AVG
SAR	1.01	2.93	7.30	0.86	8.81	8.72	7.80	3.58	9.93	4.36	4.84	2.21	11.19	1.99	9.69	5.68
%Na	52.06	67.71	54.78	16.28	43.65	45.5	43.28	54.17	60.56	73.97	40.78	54.03	54.16	52.84	55.32	51.27
RSBC	0.09	0.21	3.23	2.09	-0.37	0.86	-0.79	1.18	0.77	1.06	1.79	1.48	0.22	3.08	2.42	1.22
KR	1.45	3.04	6.45	0.92	3.29	3.97	3.11	3.33	5.14	4.39	6.39	1.25	6.94	1.59	7.56	3.92
MH	6.99	12.72	40.47	41.04	8.88	12.86	10.02	29.31	16.35	33.81	26.48	5.41	23.02	2.05	32.89	20.35
PI	154.73	143.06	126.39	228.81	87.78	94.23	86.76	127.08	97.05	125.82	153.25	104.30	98.12	158.02	112.69	126.54

Table 6. Irrigation Water classification based on SAR and alkalinity hazard.

SAR	Water class	Alkalinity hazard	Percentage
<10	Excellent	S1	93.33
10-18	Good	S2	6.67
18-26	Doubtful	S3	0.0
>26	Unsuitable	S4 & S5	0.0

with the water. According to Singh et al. (2009), low sodium water (S1) can be used for irrigation on almost all soils with little danger of the development of harmful levels of exchangeable sodium; while medium sodium water (S2) will present an appreciable sodium hazard in fine textured soils with good permeability. High sodium water (S3) may produce harmful levels of exchangeable sodium in most soils and will require special soil management, including good drainage, high leaching and organic matter additions.

The range of the %Na in the groundwater in this study is between 16.28 (Sample 4) and 73.97 (Sample 10), with an average value of 51.27 (Table 5). Table 7 shows that the water ranges from excellent to doubtful for irrigation. No samples fall under water class “Good” and class “Unsuitable”. When the concentration of sodium is high in irrigation water, sodium ions tend to be absorbed by clay particles, displacing Mg^{2+} and Ca^{2+} ions. This exchange process of Na^{+} in water for Ca^{2+} and Mg^{2+} in soil reduces the permeability and eventually results in soil with poor internal drainage (Al-Tabbal and Al-Zboon, 2012). Deflocculation and impairment of soil, which reduce permeability due to high %Na in groundwater result in restricted air and water circulation during wet conditions, and such soils are usually hard when dry (Kranth, 1987; Collins and Jenkins, 1996; Saleh et al., 1999; Singh et al., 2008, 2009). Besides affecting the growth of plants directly, high levels of sodium (and other salts), which affect soil structure, permeability and aeration, indirectly also affect plant growth (Singh et al., 2008, 2009).

Sadashivaiah et al. (2008) observed that in waters having high concentration of bicarbonate, there is a tendency for calcium and magnesium to precipitate as the water is increased in the form of sodium carbonate. The concentration of magnesium in water would adversely affect the soil quality, rendering it unfit for cultivation (Venugopal et al., 2009). The high concentration of magnesium in groundwater can be attributed to dolomite, a chief mineral of sandstone and siltstone (Haritash et al., 2008). Waters with MH >50 are considered to be harmful and unsuitable for irrigation use (Szabolcs and Darab 1964; FAO/UNESCO, 1967; Singh et al., 2009).

Magnesium in water would adversely affect the soil quality, rendering it unfit for cultivation (Venugopal et al., 2009). Magnesium hardness (MH) in the groundwater in the study area ranges from 2.05 to 41.04%, with an average of 20.35% (Table 5). MH above 50 is considered to be unsuitable for irrigation (Singh et al., 2009;

Table 7. Quality of irrigation water based on %Na.

Water class	Percentage	%Na	Cl^- meq/l	SO_4^{2-} meq/l
Class 1,Excellent	6.67% (of samples)	< 20	4	4
Class 2, Good	0% (of samples)	20 – 40	4 - 7	4 - 7
Class 3,Permissible	73.33% (of samples)	40 – 60	7 – 12	7 – 12
Doubtful	20.00% (of samples)	60 – 80	12 - 20	12 - 20
Unsuitable	0.00% (of samples)	> 80	>20	>20

Brindha et al., 2014). This indicates that the entire water is safe for use for irrigation purposes. If magnesium is less than 50, then the water is safe and suitable for irrigation (Szabolcs and Darab, 1964; Al-Tabbal and Al-Zboon, 2012).

The permeability index (PI) of a soil is a function of the sodium, calcium, magnesium and carbonate in the soil (Doneen, 1964; Vasanthaiviger et al., 2010). The PI of groundwater in the study area ranges from 87.76 to 158.02, with an average value of 126.54 (Table 5). Doneen (1964), and also the World Health Organization (WHO) classified irrigation water quality into three: Class I, Class II and Class III (Brindha et al., 2014; Şen, 2015). Water of Class I and Class II with 75% of maximum permeability in the Doneen chart are considered to be good and suitable for irrigation, while Class III water is unsuitable for irrigation (Brindha et al., 2014). With regards to the PI, all the water samples fall under Class III, and are therefore unsuitable for irrigation.

The Kelley ratio (KR) is the level of Na^+ measured against Ca^{2+} and Mg^{2+} (Kelley, 1940; Paliwal, 1967). In this study, KR ranges from 0.92 to 7.56, with an average of 3.92 (Table 5). KR value more than one is generally considered unfit for irrigation (Al-Tabbal and Al Zboon, 2012). It is seen from Table 5, therefore, that the water, apart from sample 4, is unsuitable for irrigation.

A relation of alkaline earths with weak acids is expressed in terms of residual sodium carbonate (RSC) for assessing the quality of water for irrigation (Richards, 1954). It is determined as excess of $CO3^{2-}$ and HCO_3^- over that of CA^{2+} and Mg^{2+} concentration in irrigation water. It gives an overview of the permeability problems of soil when irrigated with high sodium waters rather than normal irrigation waters (Hussain et al., 2010). When the weak acids are greater than the alkaline earths, a precipitation of alkaline earths occurs in soil, which damages the permeability of soil (Rao et al., 2012; Bhuiyan et al., 2015). Gupta (1983) suggested that residual sodium carbonate (RSC) should be calculated simply as residual sodium bicarbonate (RSBC) (Mirza et al., 2014). RSBC indicates the excess concentration of HCO_3^- over Ca^{2+} (Hussain and Hussain 2004). The RSBC for the groundwater samples ranges from -0.79 to 3.23, with an average of 1.22 (Table 5). The classification of irrigation water is as given in Table 8, after Gupta and Gupta (1987). Table 8 indicates that the groundwater is safe for use as irrigation water.

Table 8. Quality of irrigation water based on RSBC

<5	Safe
5-10	Marginal
>10	Unsatisfactory

Chloride in irrigation water is the most common source of toxicity. Chloride is highly soluble in water; and because it is not absorbed or held back by soil, therefore moves readily with the soil-water, and is taken up by the crops, moves in the transpiration stream and accumulates in the leaves (Hussain et al., 2010). In the study area, chloride concentrations in groundwater vary between 0.001 and 0.008 meq/l, with evaluation rating of 1 (Christiansen and Olsen, 1973). This implies that the groundwater is excellent for irrigation, according to the classification of Scofield (1936). Again from the Scofield classification (Table 8), the sulphate content in the water also shows the water to be excellent for irrigation.

Conclusion

Investigation on groundwater in Ankpa township reveals that the water type in the area is fresh water of Na^++K^+ - HCO_3 type.

The water is good for irrigation as shown by results of sodium adsorption ratio conducted on water samples from the area. In most parts of the area the groundwater is mainly soft though moderately hard to very hard water exists in a few locations. Water from most part of the area is good for general domestic uses and may not need to be treated for hardness

The slightly low acidity in combination with TDS as well as temperature (warm) of groundwater in the presence of dissolved oxygen can make water from the area corrosive. Detailed study can still be carried out on groundwater from the area to establish complete accurate detailed corrosion potentials of the area.

CONFLICT OF INTERESTS

The authors have not declared any conflict of interests.

REFERENCES

Al-Tabbal JA, Al-Zboon KK (2012). Suitability assessment of groundwater for irrigation and drinking purpose in the northern region of Jordan. J. Environ. Sci. Technol. 5:274-290.

Ayers RS, Wescot DW (1985). Water quality for agriculture. FAO Irrigation and Drainage paper No.20 (Rev. 1), Rome.

Ayers RS, Wescot DW (1994). Water quality for agriculture. FAO Irrigation and Drainage paper, 29 Rev.1 (http://www.fao.org/DOCREP/003/T0234E00.htm.)

Back W (1961). Hydrochemical facies and groundwater flow patterns in northern part of Atlantic coastal plain. United States Geological Survey Professional Paper, 498-A. 42p.

Back W, Hanshaw BB (1965). Chemical geohydrology. Adv. Hydrosci. 1:49-109.

Bhuiyan MAH, Ganyaglo S, Suzuki S (2015). Reconnaissance on the suitability of the available water resources for irrigation in Thakurgaon District of northwestern Bangladesh. Appl. Water Sci. 5:229-239.

Brindha K, Neena Vaman KV, Srinivasan K, Sathis Babu M, Elango L (2014). Identification of surface water-groundwater interaction by hydrogeochemical indicators and assessing its suitability for drinking and irrigation purposes in Chennai, south India. Appl. Water Sci. 4:159-174.

Carroll D (1962) Rainwater as a chemical agent of Geologic processes-a review, U.S Geological Survey water supply paper 1535-G, 18p.

Christiansen JE, Olsen EC, (1973). Irrigation projects in Quatamela: Observations and Recommendations. Uta State University-USAID/Quatamela. Logan, Uta, USA.

Collins R, Jenkins A (1996). The impact of agricultural land use on stream chemistry in the middle hills of the Himalayas, Napal. J. Hydrol, 185:71-76.

Doneen LD (1964). Notes on water quality in agriculture. Published as a water Science and Engineering Paper 4001. Department of Water Science and Engineering, University of California.

Ehirim CN, Ebeniro JO, Ogwu DA (2009). A Geophysical and hydro-Physiochemical study of the impact of a solid waste landfill (SWL) in Port Harcourt municipality, Nigeria. Pacific J. Sci. Technol. 10(2):596-603.

Ezeigbo HI, Ozoko DC (1989). An evaluation of the water resources of Nsukka and environs, Anambra State, Nigeria. Water Res. 1(2):111 – 115.

FAO/UNESCO (1967). International source-book on irrigation and drainage of arid lands in relation to salinity and alkalinity. SS.67/D.55/A, 660p.

Fipps G (1969). Irrigation water quality standards and salinity management strategies. Texas A & M AGRILIFE EXTENSION, B – 1667 4-03, 18 p.

Freeze RA, Cherry JA (1979). Groundwater, Prentice-Hall. Inc., Englewood Cliffs, New Jersey, 604 p.

George PR (1983). Agricultural water quality criteria, irrigation aspects. Resource management technical report number 30, Government of western Austeria ISSn-0729-3135.

Gibbs RJ (1970). Mechanisms controlling world water chemistry. Science 170:1088-1090.

Gupta SK (1983) Variations of water table in Yamuna grainage basin of Haryana – implications and management strategies. Paper presented at the Seminar on Strategies for Irrigation Water Management, Patna.

Gupta SK, Gupta IC (1987) Management of saline soils and waters. Oxford and IBH Publishing Company, New Delhi.

Hagras MA (2013). Water quality assessment and hydrochemical characteristics of groundwater in Punjab, Pakistan. Int. J. Res. Rev. Appl. Sci. 16(2):254-262.

Haritash AK, Kaushik CP, Kaushik A, Kansal A, Yadav AK (2008). Suitability assessment of groundwater for drinking, irrigation and industrial use in some North Indian villages. Environ. Assess. 145:397-406.

Hem JD (1985). Study and interpretation of the chemical characteristics of natural water. United states geological survey water supply paper 2254, 244 p.

Hounslow AW (1995). Water quality data: Analysis and Interpretation. CRS Press Inc., Lewis Publishers, 397p.

Hussain G, Alquwaizany A, Al-Zarah A (2010). Guidelines for irrigation water quality and water management in the Kingdom of Saudi Arabia: an overview. J. Appl. Sci. 10(2):79-96.

Hussain I, Hussain J (2004) Evaluation of irrigation water quality of the village situated near river Kothari, Rajasthan (India). Pollut. Res. 23:561-564.

Iwena OA (2012). Essential geography for senior secondary schools. Tonad Publishers limited, Lagos, Nigeria, 352 p.

Johnson EE (1975). Groundwater and Wells. Johnson Division, UOP Inc., UOP Inc., Saint Paul, Minnesota 440p.

Kacmaz H, Nakoman ME (2010). Evaluation of shallow groundwater quality for irrigation purposes in the Koprubasi uranium rae (Manisa, Turkey). BALWOIS. 25:1-9.

Kelley WP (1940). Permissible composition and concentration of irrigation water. Proc. Am. Soc. Civ. Eng. 66:607-613.

Kogbe CA (1989). The Cretaceous and Paleogene sediments of southern Nigeria. *In:* C.A.Kogbe (ed.), Geology of Nigeria. Rock View Nigeria Limited, Jos, Nigeria pp. 324-334.

Kranth KR (1987). Ground water assessment development and management. Tata McGraw-Hill Education Publ. New Delhi 720p.

Linsley RK, Franzini JB, Freyberg DL, Tchobanoglous G (1992). Water resources engineering. McGraw-Hill Series on Water Resources and Environmental Engineering, 768 p.

Mirza ATM, Rahman T, Saadat AHM, Islam SMd, Al-Mansur AMd, Ahmed S (2014). Groundwater characterization and selection of suitable water type for irrigation in the western region of Bangladesh. Appl. Water Sci. DOI 10.1007/s13201-014-0239-x, 11 p.

Misstear B, Banks D, Clark L (2006). Appendix 3 FAO Irrigation Water Quality Guidelines, in Water Wells and Boreholes, John Wiley & Sons Ltd, USA, 514 p.

Nwajide CS (2013). Geology of Nigeria's sedimentary basins. CSS Press, Lagos, 565 p.

Obaje GN (2009). Geology and Mineral Resources of Nigeria. Lecture Notes in Earth Sciences (120). Springer, Heidelberg, 221 p.

Obeta MC, Ocheja JF (2013). Assessment of Groundwater Quality in Ankpa urban Kogi state, Nigeria. Environ. Res. J. 7(3):37-47.

Obeta MC, Ocheje JF, Nwokocha VC (2015a). Analysis of the Physico-Chemical and Microbiological quality of Imabolo stream in Ankpa Urban area of Kogi state, Nigeria. Mediterr. J. Soc. Sci. 6(6 S4):549–557.

Obeta, MC, Ocheje JF, Nwokocha, VC (2015b). Effects of Land-uses on the quality of Imabolo stream in Ankpa Urban area of Kogi state, Nigeria. Acad. Interdiscip. Stud. 4(3):271-284.

Offodile ME (2002). Ground water study and development in Nigeria (2nd ed.). Mecon Geology & Eng. Services Ltd., Jos, Nigeria, 453p.

Ofoma AE, Ngah SA, Onwuka OS (2008). Salinity problems in coastal aquifers: case study from Port Harcourt, southern Nigeria. *In:* Adelana MA, MacDonald AM (eds), International Association of Hydrogeologists (IAH) selected papers on Applied Groundwater Studies in Africa, CRC Press, pp. 405-413.

Olayinka AI, Olayiwola MA (2001). Integrated use of geoelectrical imaging and hydrochemical methods in delineating limits of polluted surface and groundwater in a landfill site in Ibadan area, southwestern Nigeria. J. Min. Geol. 37(1):53-68.

Omonona OV, Onwuka OS, Okogbue CO (2014). Characterization of groundwater quality in three settlement areas of Enugu metropolis, southeastern Nigeria, using multivariate analysis. Environ. Monit. Assess. 186:651-664.

Onwuka OS, Ekwe AC, Adimonye OJ (2013b). Geoelectrical and hydrogeological assessment of the groundwater potentials of Ehandiagu, Enugu State, southeastern Nigeria. Jordan J. Earth Environ. Sci. 5(2):63-71.

Onwuka OS, Omonona OV, Anika OC (2013a). Hydrochemical characteristics and quality assessment of regolith aquifers in Enugu metropolis, southeastern Nigeria. Environ. Earth Sci. 70:1135-1141.

Onwuka OS, Uma KO, Ezeigbo HI (2004). Portability of shallow groundwater in Enugu town, southeastern Nigeria. Glob. J. Environ. Sci. 3(1):33-39.

Paliwal KV (1967). Effect of gypsum application on the quality of irrigation waters. Madras Agric. J. 59:646-647.

Rao SN (2006). Seasonal variation of groundwater quality in a part of Gunter District, Andhra Pradesh, India. J. Environ. Geol. 49:413-429.

Rao SN, Subrahmanyam A, Kumar SR, Srinivasulu N, Rao GB, Rao

PS, Reddy GV (2012) Geochemistry and quality of groundwater of Gummanampadu sub-basin., Guntur District, Andhra Pradesh, India. Environ. Earth Sci. 67(5):1451-1471.
Richard LA (1954). Diagnosis and Improvement of Saline and Alkali Soils, Agric. Handbook 60, U.S. Dept. Agric., Washington, D.C. 160pp.
Sadashivaiah C, Ramakrishnaiah CR, Ranganna G (2008). Hydrochemical analysis and evaluation of groundwater quality in Tumkur Taluk, Karnataka state, India. Int. J. Res. Public Health 5(3):158-164.
Saleh A, Al-Ruwaih F, Shehata M (1999). Hydrogeochemical processes operating within the main aquifers of Kuwait. J. Arid Environ. 42:195-209.
Schroll EE (1975). Analytshe geochemie band I methodic, Ferdinand Enke, Verlag, Stuttgart pp. 8 – 11.
Scofield FE (1936). The salinity of irrigation water. Smith. Instit. Ann. Rep. pp. 275-283.
Şen Z (2015). Practical and applied hydrogeology. Elsevier 406 p.
Singh AK, Mondal GC, Tewary BK, Sinha A (2009). Major ion chemistry, solute acquisition processes and quality assessment of mine water in Damodar valley coalfields, India. Abstract of the Mine Water Conf., Pretoria, South Africa, Proceedings ISBN Number 978-0-9802623-5-3, produced by Document Transformation Technologies cc, pp. 267-276.
Singh AK, Mondal GC. Kumar S, Singh TB. Tewary BK, Sinha A (2008), Major ion chemistry, weathering processes and water quality assessment in upper catchment of Demodar river Basin, India. Environ. Geol. 54(4):745-758.
Stuytzand PJ (1989). Hydrology and water quality aspects of Rhine bank groundwater in the Netherlands. J. Hydrol. 106(3/4):341-363.
Szabolcs I, Darab C (1964).The influence of irrigation water of high sodium carbonate content of soils. Proc. Int. Congress Trans. 2:803-812. Or Proceedings of 8th ISSS, Trans. 2:802-812.
Tijani MN (2003). Bacteriological, chemical and lithologic controls on the water quality in Shagamu area, southwestern Nigeria. J. Nig. Assoc. Hydrogeol. 14:93-100.
Todd DK, Mays LM (2005). Groundwater hydrology (3 ed.). John Wiley & Sons, Inc., New York, 636 p.
Uzoije AP, Uche CC, Uzo E, Raphael G (2015). Suitability assessment of shallow groundwater of a typical coastal aquifer for irrigation use; a water quality index model approach. IOSR J. Mech. Civil Eng. 12(6):55-60.
Vasanthaiviger M, Srinivasamoorth K, Vijayaragavan K, Rajiv Ganthi R, Chidambaram S, Anandhan P, Manivannan R, Vasudevan S (2010). Application of water quality for ground water assessment: Thirumanimuttar sub basin, Tamil Nadu, India. Environ. Monit. Assess. 171(1-4):595-609.
Venugopal T, Giridharan L, Jayaprakash M, Periakali P (2009). Environmental impact assessment and seasonal variation study of the groundwater in the vicinity of River Adyar, Chennai, India. Environ. Monit. Asses. 149:81-97.
Wang B, Wanty RB, Vohden J (2004). Geochemical process and geologic framework influencing surfacewater and sediment chemistry in the Fortymile River watershed, eastcentral Alaska. U.S. Geological Survey Professional Paper 1695, pp. 3-19.

International Journal of Physical Sciences

Related Journals Published by Academic Journals

- *African Journal of Pure and Applied Chemistry*
- *Journal of Internet and Information Systems*
- *Journal of Geology and Mining Research*
- *Journal of Oceanography and Marine Science*
- *Journal of Environmental Chemistry and Ecotoxicology*
- *Journal of Petroleum Technology and Alternative Fuels*

academicJournals